Femtosecond laser ablation for microfluidics

David Gómez
Fundación Tekniker
Av Otaola 20
20600—Eibar (Guipúzcoa), Spain
E-mail: dgomez@tekniker.es

Igor Goenaga
Fundación Tekniker
Av Otaola 20
20600—Eibar (Guipúzcoa), Spain

Ion Lizuain
Fundación Tekniker
Av Otaola 20
20600—Eibar (Guipúzcoa), Spain

Milagros Ozaita
Fundación Tekniker
Av Otaola 20
20600—Eibar (Guipúzcoa), Spain

Abstract. We present some applications of femtosecond laser ablation for microfluidics. A doubled Ti:sapphire femtosecond laser (λ=400 nm; pulse width, 90 fs; pulse energy up to 350 μJ; pulse repetition rate, 1 kHz) is used to microstructure passive microfluidic devices (channels, reservoirs, through-holes) in polymers [polymethyl methacrylate (PMMA), polyimide (PI, Kapton)] and glass (Pyrex). These materials are selected because of their extended use in the fabrication of microfluidic chips. In all cases, channels of some tenths of micrometers are obtained with a good-quality finishing for fluid transport. In the same sense, reservoirs and holes are produced. These latter elements are fabricated in larger dimensions to combine them with channels in some presented prototypes. The well-known feature of ultrashort pulses is that no edge effects are observed because the absence of thermal effects enables a good sealing. For PMMA, polymer bonding technologies are used. For Pyrex, the well-known silicon sealing by anodic bonding is chosen. In both cases, the fabricated prototypes work properly with a good flow behavior and no leakage is observed. [DOI: 10.1117/1.1902783]

Subject terms: femtosecond laser ablation; micromachining; microfluidics; bonding technologies.

Paper 040426 received Jul. 1, 2004; revised manuscript received Jan. 21, 2005; accepted for publication Jan. 27, 2005; published online May 4, 2005.

1 Introduction

The development of femtosecond laser systems has attracted great attention recently for microtechnology applications. Thus, ultrashort pulses have been successfully applied to mask fabrication (see, for example, Refs. 1 and 2), microelectromechanical systems[3] (MEMS), photonics,[4] biomedical sciences,[5,6] etc. This great development has been specially motivated by the highly reduced heat-affected zone (HAZ) shown in a material when femtosecond pulses are focused on it and ablation is produced (i.e., above the fluence threshold). Although the microscopic basics of this process are beyond the scope of this paper and still focus of controversy, it seems to be well established that absorption mechanisms in this case differ from others involved when longer pulses are used[7,8] (multiphoton ionization versus avalanche ionization). For ultrashort pulses, electron-phonon interaction ranging in the picosecond regime are minimized, and thermal effects are almost negligible.[9] Although more sophisticated models have arisen, Chichkov et al.[10] explained some experimental results by means of a two-level model. Another important characteristic of femtosecond lasers is the high peak power (>10 GW) and subsequent extremely high intensity (≈terawatts per square centimeter) achievable when focused on a spot of some micrometers in diameter. This enables efficient ablation of transparent materials[11] as well as refraction index changes that can be applied to the fabrication of optical components.[12]

Besides the pulse length, it is also well known that laser wavelength plays an important role in the minimization of HAZs. In this sense, the use of UV radiation (for example, excimers or tripled Nd:YAG lasers) instead of visible (doubled Nd:YAG) or IR (Nd:YAG, CO_2) leads to much more satisfactory results.[13] In our case, a combined effect of the just-noted features were fulfilled by using a Ti:sapphire system (τ=90 fs, λ=800 nm) that was doubled (λ=400 nm) by means of an LBO crystal. A detailed description of the equipment is given in next section.

A novel application of ultrashort laser technology consists of the fabrication of microfluidic devices. Recently, miniaturization has become an important objective in the life sciences, mainly due to the achievement of reduction costs, reagent savings, integration with electronics, portability, and disposability.[14,15] Small devices known as lab-on-chips or micro total analysis systems (μTAS) have emerged with interesting features in different fields, such as genetic and proteomic analysis, clinical diagnostics, or analytical chemistry. In most of these cases, because of the required small size of some passive components (holes, channels, reservoirs, etc.), cleanroom technologies (photolithography, plasma etching, physical or chemical vapor deposition, etc.) are required to achieve the final product or, alternatively, masters to be replicated in polymer by hot embossing or microinjection molding. These processes involve very expensive and time-consuming technology, and some authors[16,17] have used different types of lasers to suppress these drawbacks. In addition, lasers enable 2 1/2-D and 3-D micromachining that, generally, constitutes a great difficulty for planar cleanroom technologies. Taking into account the optimal features of femtosecond lasers concerning line resolution and the absence of HAZs, this technology seems to be well suited to substitute for or complement some cleanroom processes. As we show, channels and holes can be fabricated in polymers and glass with high

quality in short times. Additionally, the smooth and burr-free edges enable a good sealing of microstructures by means of bonding techniques (polymer bonding, or anodic bonding in the case of glass).

This paper focuses on the fabrication of passive microfluidic components (channels, reservoirs, and injection holes) by means of femtosecond laser machining in some transparent materials. Polymethyl methacrylate (PMMA) was chosen as a standard polymer with potential applications in this field because of its biocompatibility, low cost, thermal stability, and mechanical properties. In addition, some preliminary experiments were carried out in polyimide (Kapton). This polymer has been extensively used as a flexible material in the electric and electronic industries due to its good electrical and thermal properties (it withstands temperatures above 500°C). These interesting features have enabled it to play an important role in microfluidic applications.

Similar experiments have been performed in Pyrex glass, as another standard material commonly used in lab-on-chips fabricated to date. All the obtained structures in PMMA and Pyrex have been sealed by bonding technologies. For glass, a silicon wafer was chosen as the seal and was anodically bonded to the Pyrex. In the case PMMA, a PMMA-PMMA bonding technique was performed, and it is explained in next sections.

For all the materials, channels of some tenths of micrometers in width and depth were achieved. The obtained smooth "V" shape seems to be desirable, since it favors smooth flows without turbulent regime. In the case of PMMA and Pyrex, circular holes and reservoirs were fabricated with diameters ranging from 200 μm to 1 mm to be well scaled to channel dimensions.

2 Experimental Details

A commercial femtosecond Ti:sapphire laser system was used to perform the ablation experiments. This system is based on a femtosecond seed laser (Coherent, Vitesse LP SB) that delivers an output average power of 250 mW at a pulse repetition rate (PRR) of 80 MHz, which leads to a power peak of 35 kW and an energy peak of 3.1 nJ. Pulse width is 90 fs. This seed beam is then taken into an amplifier in multipass configuration (Quantronix, Odin-Compact DP 1.0) based on chirped pulse amplification[18] (CPA). This method enables us to increase the pulse energy up to 1 mJ at 800 nm with a PRR of 1 kHz without changing the pulse width of the seed laser after compression in the last step of the CPA. Finally, an LBO crystal is used to double the natural wavelength of the Ti:sapphire beam (λ=800 nm) by means of second-harmonic generation (SHG) techniques. The resulting beam, used to perform all the experimental tests presented in this paper, is Gaussian [beam quality, $M^2<1.5$ (TEM_{00})], circular (3 mm in diameter), UV (λ =400 nm), the maximum energy peak is 350 μJ, and repetition rate is 1 kHz. Fluence on the sample was controlled by varying the polarization plane of the beam before the LBO crystal by means of the rotation of a half-wave plate. Taking into account the polarization-dependent efficiency of second-harmonic conversion, it was possible to control energy variations from 0 mJ to 350 μJ in 1-μJ steps.

The samples for the experimental tests were placed in a computer controlled XYZ-stage positioning system from Aerotech with resolution of 0.1 μm and reproducibility (3σ) of ± 1 μm in the case of the XY stages and 0.5 μm and ± 2 μm, respectively, for the Z stage. A circular mask (2 mm in diameter) was used before focusing the beam on the sample to remove the tails of the Gaussian profile. A fused silica planoconvex lens with a focal length of 100 mm (Newport, SPX022) was used as the focusing optics. In all cases, the focal point was focused on the surface of the sample and no image projection techniques were used. Additionally, experiments were carried out in open air and a nitrogen blow was used for debris removal when machining. Pyrex glass wafers (4 in., 0.5 mm thick) were commercially acquired from Plan Optik, PMMA foils (0.5 mm thick) from Bayer, and PI (Kapton, 0.125 mm thick) from Goodfellow.

For bonding, an EVG501 manual wafer bonding system from EVG Systems was used. The system operates in a vacuum chamber (10^{-4} mbars), and can reach contact forces up to 3.5 kN, temperatures from 20 to 550°C, and applied voltages from 0 to 2000 V at 50 mA. In the case of PMMA, a combination of a thermal cycle synchronized with a force cycle was used for polymer bonding. For Pyrex glass, electric voltage was also applied in the usual anodic bonding process.[19] More details about the processes developed in this paper are provided in next section.

The characterization of fabricated devices was carried out by means of a confocal microscope composed by a Nikon ME600P optical microscope, a piezoelectric system placed in the XY stage, and acquisition and measure software. In this way, it is possible to measure widths and depths with a resolution of 0.18 μm in the XY plane and below 10 nm on the Z axis. In addition, scanning electron microscopy (SEM) and conventional optical microscopy were used to visualize some of the fabricated structures.

3 Results and Discussion

As noted in the introduction, the final goal of this paper consists of the development of some microfluidic devices as a demonstrator of femtosecond laser ablation capabilities for this kind of application. As an example of the process followed for the consecution of this purpose, Fig. 1 depicts the main steps carried out in the fabrication of a simple device similar to others presented in this section. First, a channel microstructure is ablated in the upper side of the sample and through-holes are made at the end of each. After this, the sample is cleaned and the ablated side is sealed to avoid leakage. In this way, sealed structures are obtained and ready to use for storing or causing liquids to flow. Although this paper aims to show the capabilities of ultrashort lasers for microfluidics and only some simple devices are shown as demonstrators, the stacking of different aligned layers can lead to more complicated designs. The different processed materials are shown and results are commented on.

3.1 *Pyrex Glass*

For channels in Pyrex glass, the first experiments were carried out at a fluence of 5.5 J/cm^2. For this value, the width and depth of the channels was controlled by means of the number of pulses. Taking into account that the sample is

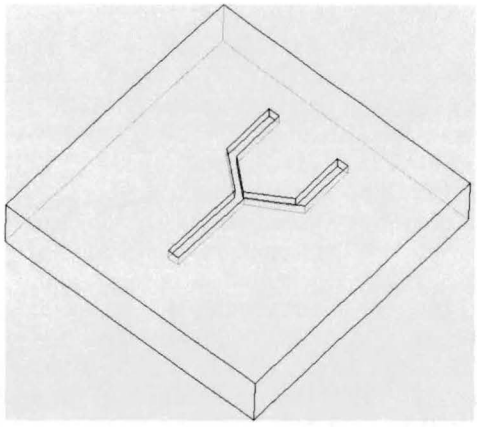

(a)

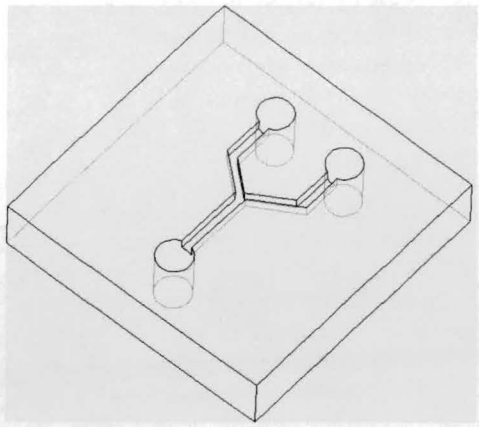

(b)

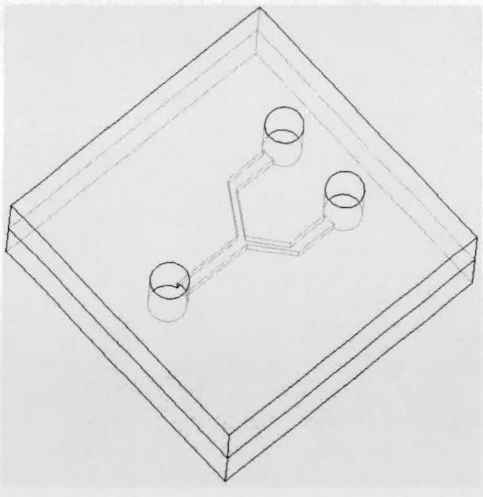

(c)

Fig. 1 Schematic sequence followed in this paper for the fabrication of microfluidic devices: (a) femtosecond laser ablation of the channels, (b) through-holes, and (c) sealing; (c) was turned with respect to the others to show the final aspect of the microfluidic device.

moving at a given feedrate f in the horizontal plane, and that the spot diameter s is known, it is easy to calculate that the number of pulses in a radiated part of the sample N by the following expression:

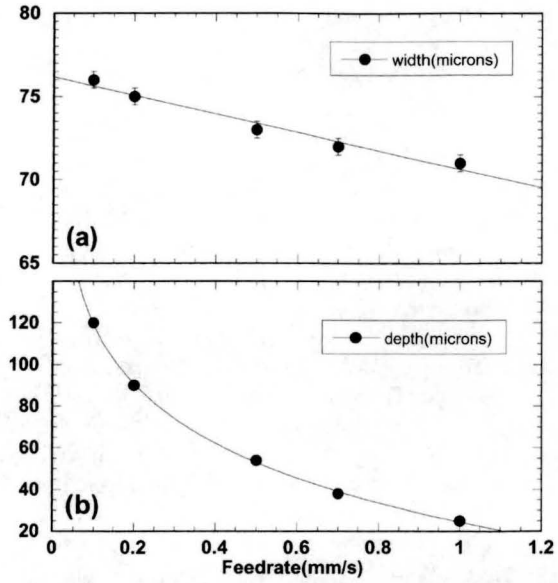

Fig. 2 (a) Width and (b) depth dependence of the feedrate of the XY stages for Pyrex glass with an irradiation fluence of 5.5 J/cm^2: solid lines represent linear and logarithmic fittings, respectively.

$$N = \frac{s(\text{mm})\text{PRR(Hz)}}{f(\text{mm/s})}, \tag{1}$$

where PRR represents the pulse repetition rate. Figure 2 shows the values obtained for 5.5 J/cm^2. Some conclusions can be extracted.

The channel width seems to change smoothly in the feed rate range. Therefore, to control this magnitude in the desired range (some tenths of micrometers), not only this parameter should be taken into account but also fluence must be considered. Widths of 60 and 31 μm for fluences of 3.5 and 1.5 J/cm^2, respectively, were obtained for a feedrate of 500 μm/s. This result is in agreement with the logarithmic behavior of fluence with the square of spot size for Gaussian beams.

As expected, the final depth of the channel clearly depends on the feed rate. In the tested range (from 100 μm/s to 1 mm/s) this dependence can be well fitted to a logarithmic behavior. When fluence is considered, the well-known fluence logarithmic dependence (for example, depths of 45 and 20 μm for 3.5 and 1.5 J/cm^2, for a feed rate of 500 μm/s) is observed. Taking Eq. (1) into account, this dependence can be also expressed as function of the number of pulses.

After this study, it was possible to microstructure a channel of a desired width and depth. As an example, we aimed to microstructure channels with a width of 60 μm and a depth of 30 μm. According to previous results, a fluence of 3.5 J/cm^2 and a feed rate of 800 μm/s were chosen. Figure 3(a) shows the obtained microfluidic channels with a width of 59 μm and a depth of 32 μm. Similar results were obtained in other tests and it is possible to establish an error below 5 μm in all cases. Figure 3(b) shows a spherical microfabricated reservoir with a diameter of 1 mm and a depth of 257 μm.

For holes, diameters from 200 μm up to 1 mm were manufactured. As a first attempt, percussion drilling was

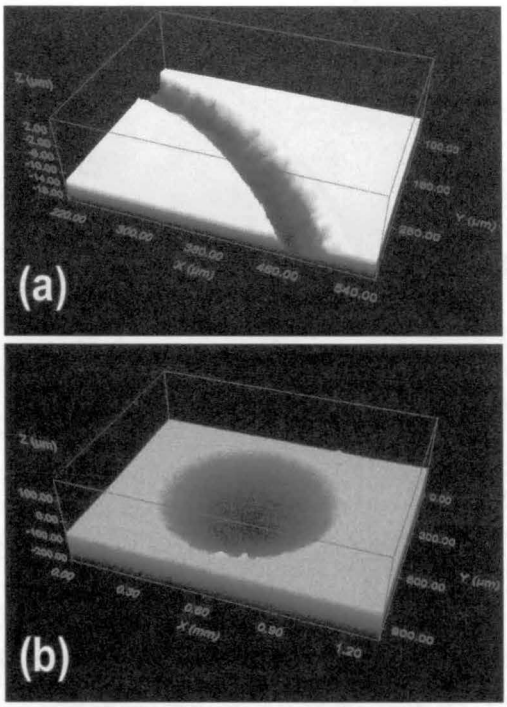

Fig. 3 (a) 3-D confocal mapping of a Pyrex channel 58 μm wide and 29 μm deep and (b) a circular reservoir (diameter of 1 mm) 257 μm deep.

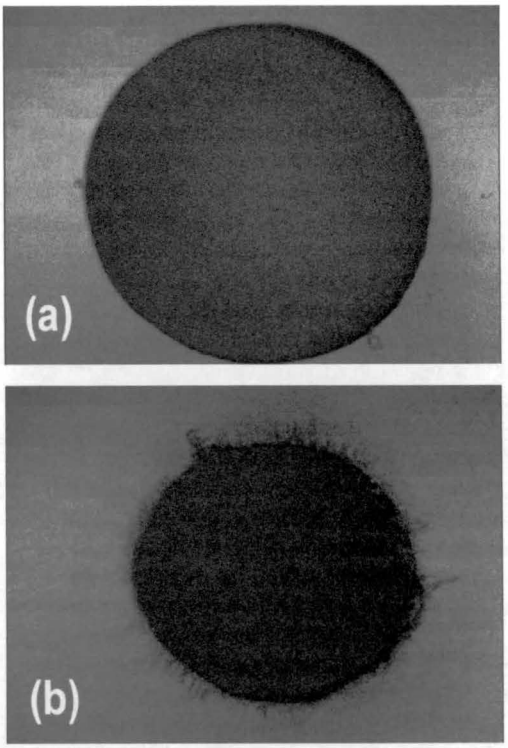

Fig. 4 (a) Entrance and (b) exit hole in 0.5-mm-thick Pyrex. The entrance hole has an average diameter of 501 μm and the exit diameter is 398 μm.

selected, although, as noted by some authors,[13,19] this technique leads to unsatisfactory results in terms of roundness and edge finishing. A much more efficient process in this sense is achieved by trepanning. The use of a spot with a small size, which was previously well characterized, enabled good results for holes of some hundreds of micrometers. The trepanning method has been optimized for our case, and three concentric channels instead of only one, as in conventional trepanning, led to more satisfactory results, especially when microcracks were to be avoided. Figure 4 shows, as an example, one hole fabricated by this optimized trepanning and the percussion method. As we can see, the exit hole (diameter: 398 μm) is smaller that the entrance hole (diameter: 501 μm), due to the taper angle usually observed in ablation processes. We can see that even in this case, microcracks of some micrometers are still present. Taking into account the thickness of the Pyrex wafer (500 μm), the estimated angle is 84.1 deg. Figures 3 and 4 show burr-free edges, with no visible HAZ and no deposited debris. The wall roughness was measured by means of confocal microscopy. Table 1 shows some root mean square (rms) values corresponding to feed rates and fluences similar to those used in this paper. We can observe a small decrease of roughness with increasing feed rate. No clear effect of fluence on this parameter is noticeable, within the experimental uncertity. In a sense similar to that for channels and holes, reservoirs represent an important element in microfluidics when we intend to store fluids to be dispensed. The fabricated reservoirs were fabricated with a spherical shape, which could be obtained by controlling the number of laser passes.

To seal the microstructured glass, a silicon wafer lid was used and the well-known anodic bonding technique was applied.[20] Both wafers were cleaned and placed in the chamber, which was heated up to 350°C and pumped to a vacuum of 10^{-4} mbar. A force of 500 N and a voltage cycle with values up to 800 V were then applied for 20 min. The chamber was then brought back to atmospheric pressure and cooled down, leading to a very strong, almost irreversible bond.

Finally, Fig. 5 shows a microstructured Pyrex wafer with four different micromachined devices sealed to a plain silicon wafer. In all cases, liquid was introduced using one of the holes as an entrance by means of an automated syringe system. A constant liquid flow was observed along the four tested devices.

3.2 *Polymethyl Methacrylate (PMMA)*

In a manner similar to that for Pyrex glass, microfluidic devices were fabricated in PMMA sheets and then sealed to other plain sheets. Before performing these devices, a study

Table 1 Obtained roughness values (rms) for different feed rates and fluences for Pyrex and PMMA with values given in micrometers.

	Pyrex		PMMA	
	$F=4.0$ J/cm^2	$F=5.5$ J/cm^2	$F=0.55$ J/cm^2	$F=0.76$ J/cm^2
$f=0.2$ mm/s	0.478	0.514	0.674	0.724
$f=0.5$ mm/s	0.376	0.365	0.583	0.601
$f=1$ mm/s	0.247	0.302	0.556	0.589

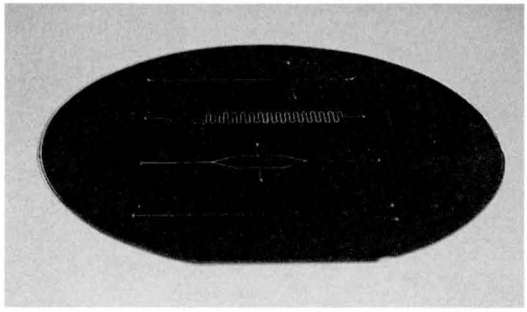

Fig. 5 Picture of a 4-in. Pyrex wafer with four different microfluidic structures bonded to a 4-in. plain silicon wafer.

of femtosecond laser ablation of PMMA has been carried out, as was done before for Pyrex. After some coarse tests, it was concluded that, for this material, lower fluences are required if channel widths and depths in the 40- to 100-μm range are required. In this way, for the desired dimensions in width and depth, fluences below 1 J/cm^2 should be considered. For higher values, surface finishing is not good enough and depths are of a dimension similar to sheet thickness.

For this material, a design of experiments was performed and 12 channels were microstructured corresponding to three different fluences (0.76, 0.65, and 0.55 J/cm^2) and four feed rates (100, 200, and 500 μm/s and 1 mm/s). Figure 6 shows the results obtained for channel width and depth. In the first case, a difference of approximately 22% in width is observed from the fastest to the slowest feed rates. This value is clearly higher that the one obtained for Pyrex, where the difference was around 10%. The tested range in fluence and feed rate ensures the control of channel width in the desired values for this work. Concerning depth, the logarithmic behavior of the inverse of feed rate (similar to number of pulses) is also achieved in PMMA for all the fluences. In Figs. 6(b) and 7, the ablation depth is represented as function of feed rate and fluence, respectively. Taking into account the commented $d \propto \log(1/f)$ law for the feed rate and the known logarithmic behavior for fluence, a minimization procedure was carried out to model the $d(f,F)$ curve. In this way, the curve

$$d(f,F) = 640.08 \log\left(\frac{2.74}{f}\right) \log\left(\frac{F}{0.355}\right), \tag{2}$$

where d is expressed in micrometers, f in millimeters per second, and F in joules per square centimeter, gives account of depth behavior with high accuracy in the measured range (regression factor: 0.997). The solid lines in Figs. 6(b) and 7 correspond to Eq. (2). The limiting value $f_0 = 2.74$ mm/s has no physical meaning and the feed rate dependence should not be extrapolated in any case from the studied values. Concerning fluence dependence, a fluence threshold value of $F_0 = 0.355$ J/cm^2 was extracted.

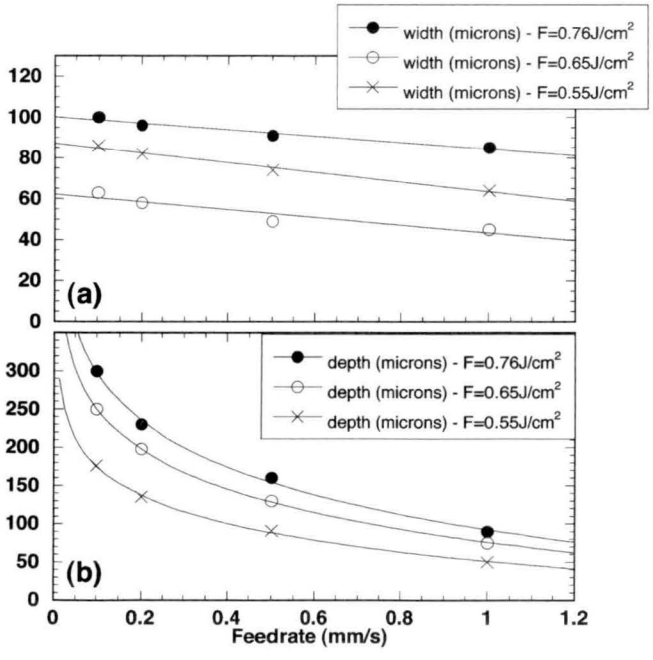

Fig. 6 (a) Width and (b) depth dependence of the feedrate of the XY stages for PMMA with an irradiation fluence of 0.55, 0.65, and 0.76 J/cm^2; solid lines represent linear and logarithmic fittings, respectively.

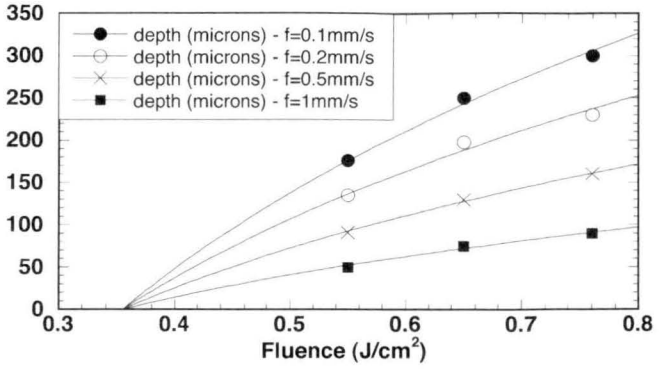

Fig. 7 Depth as function of fluence for different feed rates. Solid lines represent fittings to Eq. (2) in the text.

As in the case of Pyrex glass, the study carried out enabled us to control process conditions to obtain channels with defined widths and depths. Again, errors below 5 μm were obtained for this polymer. An example is shown in Figs. 8(a) and 8(b), where a channel with an aspect ratio equal to unity (width and depth equal to 100 μm) was desired. For $f = 1$ mm/s and $F = 0.81$ J/cm^2 it was possible to obtain $w = 102$ μm and $d = 97$ μm. As we can see in Fig. 8(b), the channels have well-defined edges with neither HAZ nor burr. As in the case of Pyrex, roughness rms results are shown in Table 1. The same behavior concerning feed rate and fluence dependence is observed. Concerning PMMA through holes, microcracks are not so noticeable, although they are also present due to the brittle nature of this polymer.

Laser micromachined PMMA was bonded to plain PMMA sheets following the solvent-assisted bonding method described in Ref. 17. Both sheets were cleaned in ethanol, and then heated to 110°C and pressed together with a force of 2000 N for 30 min in the bonder sys tem. The bonded structure was then cooled down to 80°C while the force was still applied. It is crucial to keep the bonding temperature slightly below PMMA glass tran-

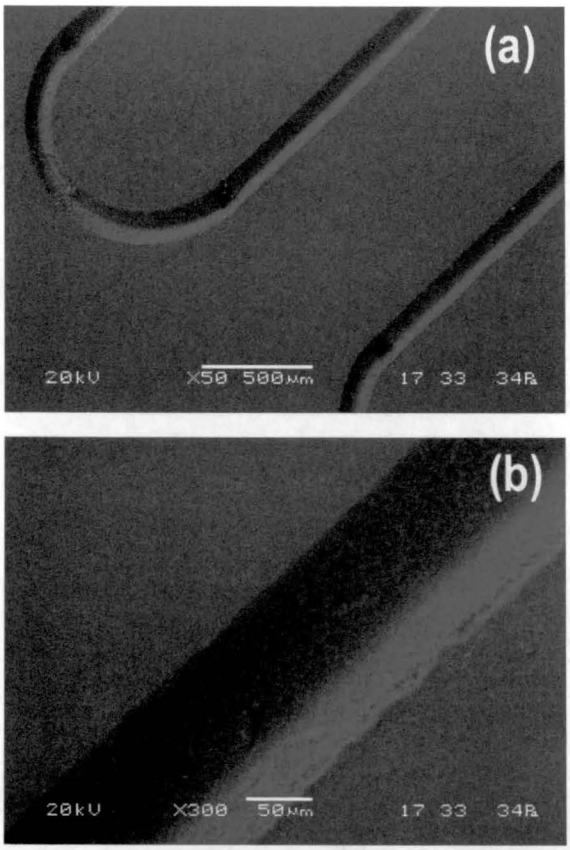

Fig. 8 SEM images of 102-μm-wide and 97-μm-deep PMMA channels: (a) general view and (b) detail of the channel profile.

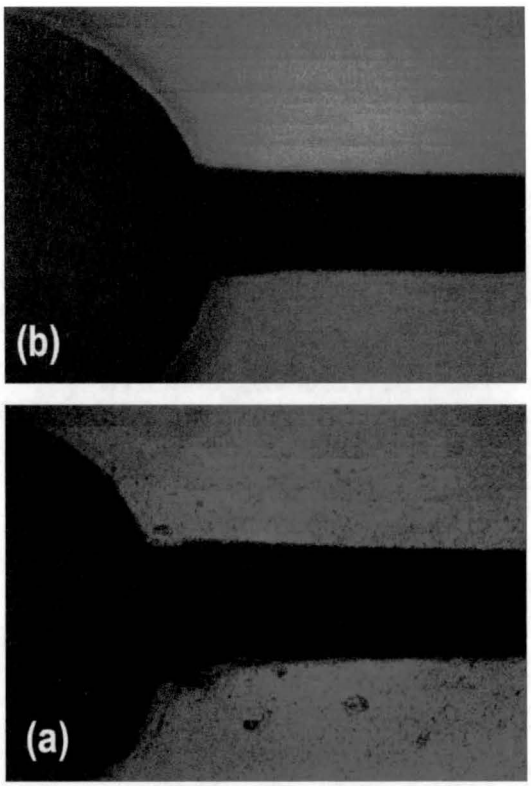

Fig. 9 Junction channel-hole in PMMA (a) before and (b) after sealing; a slight deformation can be seen.

sition temperature, i.e., $T_g \sim 115°C$, to avoid the channel collapsing due to the softening of PMMA at these temperatures. The bond strength achieved with this method is not too high, meaning that it is reversible, but it is still enough to obtain completely sealed microchannels. The main difficulty of this step consists of the accuracy required in the temperature-time cycle, because the process could lead to the deformation of the channels due to PMMA flowing. In fact, although all the processes were carried out some degrees below the glass transition of the polymer, some thermal effects were observed in the polymer (glass transition does not represent a sharp limit). After optimizing the sealing process, these deformations were measured by means of optical microscopy. It was observed that the cases where deformation is higher correspond to areas of the device where the polymer has more free space in which to flow (i.e., channel-reservoir or channel-hole junctions). As an example, Fig. 9 shows a hole-channel junction before [Fig. 9(a)] and after [Fig. 9(b)] sealing. We can clearly see a smooth deformation of the channel, which is especially noticeable close to the hole. The estimated highest values of deformation are below 5 μm. Some of the fabricated devices are presented in Fig. 10. They were tested for fluid transport and, as is clearly seen in Fig. 11, liquid flow is attained without leaking in the serpentine structure. Similar results were obtained for the four structures tested (the same ones as in Pyrex glass).

3.3 *Polyimide*

Some preliminary results have been recently obtained in polyimide (PI). In the same manner as for the two preceding materials, the femtosecond ablation process of this material is still being studied and no final results are presented in this paper. As a general outline, it can be said that the same kind of behavior observed for Pyrex and PMMA was found here for width and depth of channels. Up to now, no experiments have been carried out concerning the fabrication of microfluidic structures and subsequent bonding. Figure 12 shows some of these preliminary results for PI, where channels with $\omega = 35$ μm and $d = 30$ μm were obtained for $f = 500$ μm/s and $F = 1.6$ J/cm^2.

4 Discussion and Final Conclusions

As was shown in this paper, we can conclude that femtosecond laser ablation constitutes an interesting tool for the fabrication of microfluidics devices when it is combined with bonding technologies. This is mainly due to its almost null HAZ, burr-free edges, and no debris deposition. These features enable a good sealing of passive microfluidic components. Other important characteristics of this process are its capability to micromachine any kind of material, after getting empirically the $\omega(f,F)$ and $h(f,F)$ characteristic curves, and its high processing speed. Although the work was focused on dimensions from some tenths (for channels) to hundreds of micrometers (for through-holes and reservoirs), dimensions of few micronmeters are also easily attainable. Although only passive components were shown, actually these are being assembled in more complex fluidic

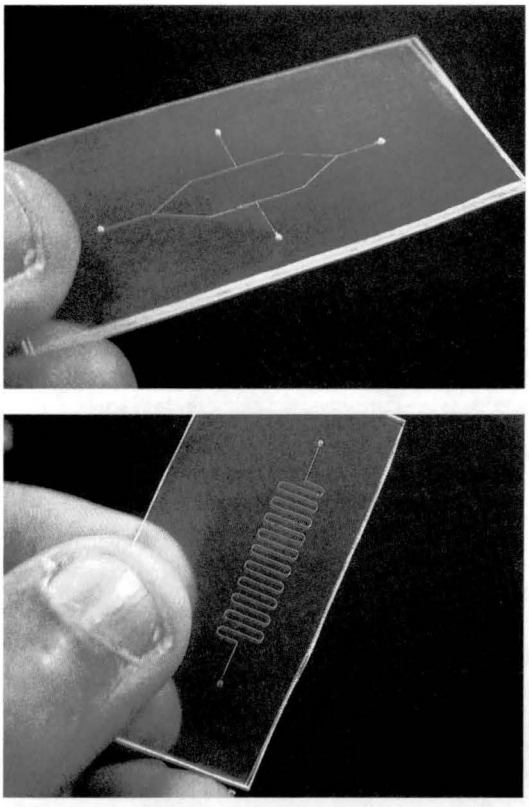

Fig. 10 Two examples of simple microfluidic devices fabricated in PMMA by femtosecond and polymer bonding technology.

devices as dispensers and lab-on-chips. Some work in this sense is intended to be presented in a near future.

This method constitutes an interesting alternative to other technologies to fabricate microfluidic devices and it can also complement them. In this sense, some cleanroom technologies can be substituted for by this femtosecond laser when no submicrometer resolution is required. Even in that case, for Pyrex-silicon chips, submicrometer features can be well made in silicon by means of electron beam lithography, ion-focused beam, plasma etching, etc. and micrometric features in glass can be made by femtosecond laser ablation. After these two processes only an alignment procedure is required before bonding. This hybrid method constitutes an interesting technique since the high costs and time usually involved in cleanroom technologies can be avoided.

Concerning polymer fabrication of microfluidic devices, in addition to the direct ablation presented in this paper, replication methods are required when mass-production is desired. In general, the extensively known LIGA technology[21] [a German acronym derived from the words lithographie, galvanoformung (electroplating) and abformung (molding)] constitutes a very expensive replication method since x-Ray lithography is involved. Thus, related technologies (DEEMO, UV-LIGA, etc.) known as LIGA-like processes have arisen for the manufacture of metal molds to be replicated in polymer when no submicrometer resolution is required. As a main conclusion, we can say that these technologies should overcome femtosecond laser ablation only when high resolution and/or a high production is necessary. Even in this case, femtosecond laser ablation could be a good choice as an inexpensive fabrication method for prototyping, preceding the manufacturing of highly expensive and time-consuming molds.

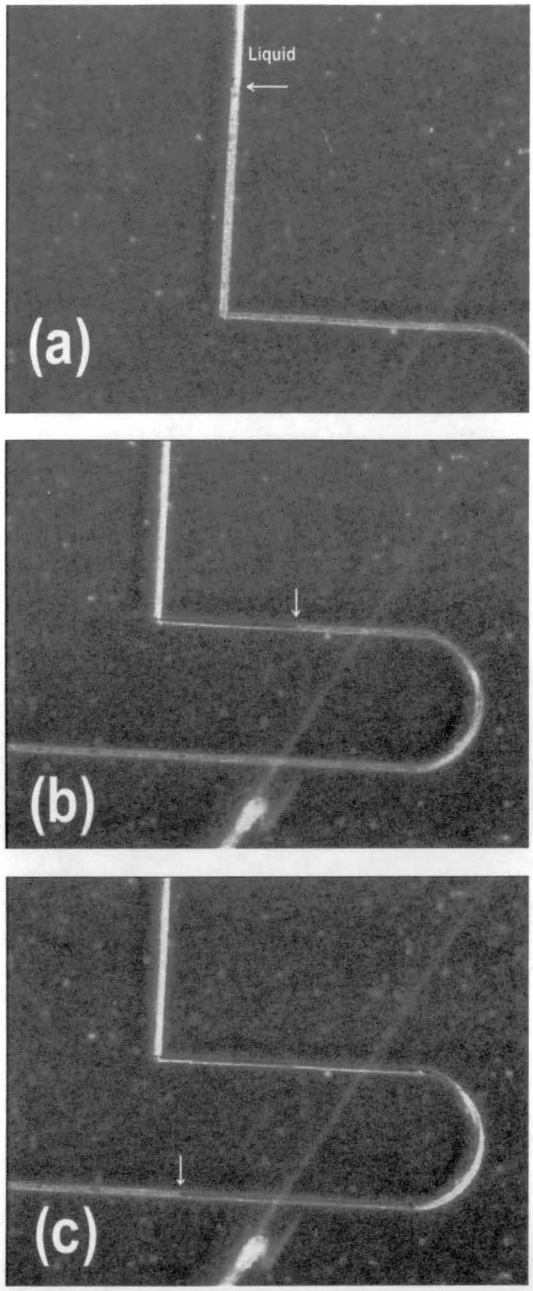

Fig. 11 Sequence of tinted liquid (in red, white arrow) flowing in one of the microfluidic devices made in PMMA. The width of the channel is 50 μm and the depth is 35 μm.

These techniques are most often highly costly in price and time, since cleanroom technologies are required. In addition, the processes do not enable 3-D fabrication, and difficult 2 1/2-D alternatives have also been used when required. To avoid these difficulties, some new laser-LIGA methods are becoming more and more interesting since they can solve some of the noted problems. In this way, the use of femtosecond lasers for mold manufacturing of microfluidic devices represents an important alternative to be investigated.

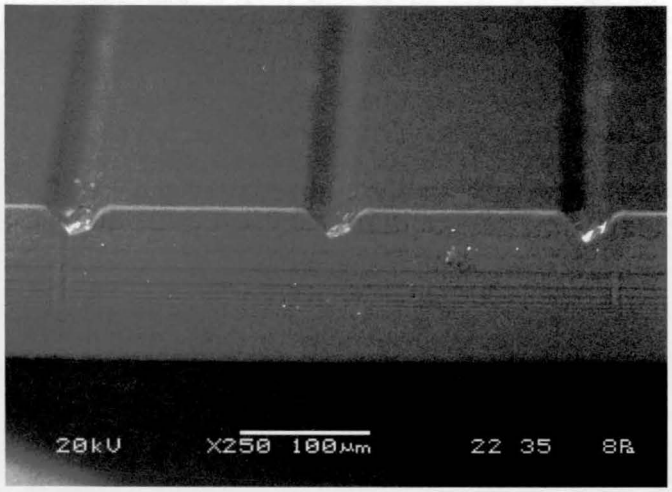

Fig. 12 SEM image of polyimide channels with a width of 35 μm and a depth of 30 μm micromachined at a fluence of 1.6 J/cm^2 and a feed rate of 500 μm/s.

References

1. S. M. Metev and V. P. Veiko, in *Laser Assisted Microtechnology, 2nd Edition*, R. M. Oswood, Ed., pp. 76–79, Springer-Verlag, Germany (1998).
2. P. Stanley, K. Venkatakrishnan, and L. Lim, "Influence of femtosecond laser parameters on the fabrication of photomask by direct ablation," *Lasers Eng.* **13**(1), 13–23 (2003).
3. R. Fedosejevs, M. Argument, A. Sardarli, S. E. Kirkwood, R. Holenstein, and Y. Y. Tsui, "Laser micromachining for microfluidic, microelectronic and MEMS applications," in *Proc. Int. Conf. on MEMS, NANO and Smart Systems*, July 20−23, Banff, Alberta, Canada, p. 53 (2003).
4. P. R. Herman, K. P. Chen, P. Corkum, A. Naumov, S. Ngi, and J. Zhang, "Advanced lasers for photonic device microfabrication," *RIKEN Rev.* **32**, 31–35 (2001).
5. C. Momma, U. Knop, and S. Nolte, "Laser cutting of slotted tube coronary stents—state-of-the-art and future developments," *Progr. Biomed. Res.* **4**(1), 39−44 (1999).
6. J. Servin, T. Bauer, and C. Fallnich, "Femtosecond lasers as novel tool in dental surgery," *Appl. Surf. Sci.* **197**, 737–740 (2002).
7. P. P. Pronko, S. K. Dutta, J. Squier, J. V. Rudd, D. Du, and G. Mourou, "Machining of sub-micron holes using femtosecond laser at 800 nm," *Opt. Commun.* **114**, 106−110 (1995).
8. A. Kaiser, B. Rethfeld, M. Vicanek, and G. Simon, "Microscopic processes in dielectrics under irradiation by subpicosecond laser pulses," *Phys. Rev. B* **61**(17), 11437–11450 (2000).
9. Y. Hosokawa, M. Yashiro, T. Asahi, and H. Masuhara, "Dynamics and mechanism of discrete etching of organic materials by femtosecond laser excitation," in *Laser Applications in Microelectronic and Optoelectronic Manufacturing VI, Proc. SPIE* **4274**, 78–87 (2001).
10. B. N. Chichkov, C. Momma, S. Nolte, F. Von Alvensleben, and A. Tünnermann, "Femtosecond, picosecond and nanosecond laser ablation of solids," *Appl. Phys. A: Solids Surf.* **63**, 109–115 (1996).
11. I. V. Hertel, "Surface and bulk ultrashort pulsed laser processing of transparent materials," *Proc. SPIE* **4088**, 17–24 (2000).
12. K. Yamada, W. Watanabe, K. Kintaka, J. Nishii, and K. Itoh, "Fabrication of volume grating induced in silica glass by femtosecond laser," *Proc. SPIE* **5063**, 474–477 (2003).
13. T. Abeln, J. Radtke, and F. Dausinger, "High precision drilling with short pulsed solid-state lasers," in *Proc. Laser Microfabrication Conf. ICALEO 99*, November 15−17, Orlando, Florida, Vol. 88, pp. 195–203 (2000).
14. B. H. Weigl and P. Yager, "Microfluidic diffusion-based separation and detection," *Science* **283**, 346−347 (1998).
15. L. J. Kricka, "Miniaturization of analytical systems," *Clin. Chem.* **44**, 2008–2014 (1998).
16. M. A. Roberts, J. S. Rossier, P. Bercier, and H. Girault, "UV laser machined polymer substrates for the development of microdiagnostic systems," *Anal. Chem.* **69**, 2035–2042 (1997).
17. H. Klank, J. P. Kutter, and O. Geschke, "CO_2 laser micromachining and back-end processing for rapid production of PMMA-based microfluidics systems," *Lab Chip* **2**, 242–246 (2002).
18. G. Chériaux and J. P. Chambaret, "Ultra-short high intensity laser pulse generation and amplification," *Meas. Sci. Technol.* **12**, 1769–1776 (2001).
19. C. Föhl, D. Breitling, K. Jasper, J. Radtke, and F. Dausinger, "Precision drilling of metals and ceramics with short and ultrashort pulsed solid-state lasers," *Proc. SPIE* **44261**, 104−107 (2002).
20. E. Obermeier, "Anodic wafer bonding," in *Proc. 3rd Int. Symp. on Semiconductor Wafer Bonding: Science, Technology and Applications*, Vol. 95-7, pp. 212−220, The Electrochemical Society, Pennington, NJ (1995).
21. J. Hruby, "LIGA technologies and applications," *MRS Bull.*, pp. 1−4 (Apr. 2001).

David Gómez received his degree in physics in 1993 from the Universidad de Cantabria, Spain, where until 1996, he was an assistant researcher with the Condensed Matter Department. In 2000 he received his PhD degree from the Universidad del País Vasco, Spain, related to the physical properties of amorphous polymers close to the glass transition. He joined the Micro- and Nanotechnology Department of the Fundación Tekniker in 2001, where he has been involved in cleanroom technologies (photolithography, plasma etching, etc.). Since 2003, his work has focused on the application of femtosecond phenomena to micromachining applications.

Igor Goenaga received his mechanical engineering degree from the Industrial Engineering School, the Universidad de Navarra, Spain, in 1999 and his MSc degree in precision engineering from Cranfield University, England, in 2002. Since 2002 he has been with the Micro- and Nanotechnology Department of the Fundación Tekniker, working in the field of femtosecond laser micromachining of different materials.

Ion Lizuain studied physics at the Universidad del País Vasco, Spain, and the University of Copenhagen, Denmark, with an orientation to solid state physics, and graduated in 2003. Since October 2003, he has been working on microelectromechanical systems (MEMS) fabrication in the Department of Micro- and Nanotechnologies, Fundación Tekniker, focusing his work on wafer bonding technologies.

Milagros Ozaita received her degree in physics in 1986 from the Universidad Complutense de Madrid, Spain, and her master of engineering science degree in 1995 from the Penn State University, United States. From 1988 to 2002, she was with the Spanish Army Research Center, Penn State University, and Lucent Technologies, involved in plasma processes and cleanroom technologies. In 2003 she become a researcher in these technologies at Fundación Tekniker.